Chaotic inflation, radiative corrections and precision cosmology

V. Nefer Şenoğuz*
Division of Sciences, Doğuş University, 34722 Kadıköy, Istanbul, Turkey

Qaisar Shafi†
Bartol Research Institute, Department of Physics and Astronomy, University of Delaware, Newark, DE 19716, USA

We employ chaotic (ϕ^2 and ϕ^4) inflation to illustrate the important role radiative corrections can play during the inflationary phase. Yukawa interactions of ϕ, in particular, lead to corrections of the form $-\kappa\phi^4\ln(\phi/\mu)$, where $\kappa > 0$ and μ is a renormalization scale. For instance, ϕ^4 chaotic inflation with radiative corrections looks compatible with the most recent WMAP (5 year) analysis, in sharp contrast to the tree level case. We obtain the 95% confidence limits $2.4\times10^{-14} \lesssim \kappa \lesssim 5.7\times10^{-14}$, $0.931 \lesssim n_s \lesssim 0.958$ and $0.038 \lesssim r \lesssim 0.205$, where n_s and r respectively denote the scalar spectral index and scalar to tensor ratio. The limits for ϕ^2 inflation are $\kappa \lesssim 7.7\times10^{-15}$, $0.929 \lesssim n_s \lesssim 0.966$ and $0.023 \lesssim r \lesssim 0.135$. The next round of precision experiments should provide a more stringent test of realistic chaotic ϕ^2 and ϕ^4 inflation.

PACS numbers: 98.80.Cq

arXiv:0806.2798v3 [hep-ph] 5 Sep 2008

Chaotic inflation driven by scalar potentials of the type $V = (1/2)m^2\phi^2$ or $V = (1/4!)\lambda\phi^4$ provide just about the simplest realization of an inflationary scenario [1]. For the ϕ^2 potential, the predicted scalar spectral index $n_s \approx 0.966$ and scalar to tensor ratio $r \approx 0.135$ are in good agreement with the most recent Wilkinson Microwave Anisotropy Probe (WMAP) 5 year analysis [2, 3]. For the ϕ^4 potential, the predictions for n_s and r lie outside the WMAP 95% confidence limits.

In this letter we wish to emphasize the fact that radiative corrections can significantly modify the 'tree' level predictions listed above. The inflaton field ϕ must have couplings to 'matter' fields which allow it to make the transition to hot big bang cosmology at the end of inflation. These couplings will induce quantum corrections to V, which we take into account following the analysis of Coleman and Weinberg [4]. (For a comparison of Coleman-Weinberg potential with WMAP, see Ref. [5].) Even if such terms are sub-dominant during inflation, they can make sizable corrections to the tree level predictions for n_s and r.

Here, we investigate the impact of quantum corrections on the simplest chaotic (ϕ^2 and ϕ^4) inflation models. We do not consider a specific framework such as supergravity, where the potential generally gets modified and becomes exponentially steep for super-Planckian values of the field. (For a realization of chaotic inflation in supergravity, see Ref. [6].) We instead assume that quantum gravity corrections to the potential become large only at super-Planckian energy densities [7], which can allow higher order terms to be negligible during the observable part of inflation [8]. We are mainly interested in the coupling of ϕ to fermion fields, for these give rise to radiative corrections to V which carry an overall negative sign. A simple example is provided by the Yukawa coupling $(1/2)h\phi\bar{N}N$, where N denotes the right handed neutrino. (Note that N may also have bare mass terms.) Such couplings provide correction terms to V which, to leading order, take the form

$$V_{\rm loop} \approx -\kappa\phi^4 \ln\left(\frac{h\phi}{\mu}\right) \tag{1}$$

where $\kappa = h^4/(16\pi^2)$ in the one loop approximation, and μ is a renormalization scale. The negative sign is a characteristic feature for the contributions from fermions.

By taking into account the contribution provided by Eq. (1), we find that depending on κ, the scalar to tensor ratio r can be considerably lower than its tree level value. An interesting consequence is that ϕ^4 inflation, which has been ruled out at tree level, becomes viable for a narrow range of κ. The predictions for n_s and r extend from the tree level values to a new inflation regime of small r and $n_s \ll 1$. (A similar range of predictions can be obtained at tree level for the binomial potential $V = V_0 - (1/2)m^2\phi^2 + (1/4!)\lambda\phi^4$ [9].) We can expect that the next round of precision measurements of n_s, r and related quantities such as $\alpha \equiv {\rm d}n_s/{\rm d}\ln k$ will provide a stringent test of these more realistic ϕ^2 and ϕ^4 inflation models.

To see how the correction in Eq. (1) arise, consider the Lagrangian density

$$\begin{aligned}\mathcal{L} = &\frac{1}{2}\partial^\mu\phi_B\partial_\mu\phi_B + \frac{i}{2}\bar{N}\gamma^\mu\partial_\mu N - \frac{1}{2}m_B^2\phi_B^2 - \frac{\lambda_B}{4!}\phi_B^4 \\ &- \frac{1}{2}h\phi_B\bar{N}N - \frac{1}{2}m_N\bar{N}N\,,\end{aligned} \tag{2}$$

where the subscript 'B' denotes bare quantities, and the field N denotes a Standard Model singlet fermion (such

*Electronic address: nsenoguz@dogus.edu.tr
†Electronic address: shafi@bartol.udel.edu

as a right handed neutrino). The inflationary potential including one loop corrections is given by

$$V = \frac{1}{2}m^2\phi^2 + \frac{\lambda}{4!}\phi^4 + V_{\rm loop}\,, \tag{3}$$

where, following Ref. [4],

$$V_{\rm loop} = \frac{1}{64\pi^2}\left[\left(m^2+\frac{\lambda}{2}\phi^2\right)^2 \ln\left(\frac{m^2+(\lambda/2)\phi^2}{\mu^2}\right) - 2(h\phi+m_N)^4\ln\left(\frac{(h\phi+m_N)^2}{\mu^2}\right)\right]. \tag{4}$$

For the range of h that we consider, $h\phi \gg m$ and $h^2 \gg \lambda$ during inflation. Also assuming $h\phi \gg m_N$, the leading one loop quantum correction to the inflationary potential is given by Eq. (1). Note that with $h\phi \gg H$ (Hubble constant), the 'flat space' quantum correction is a good approximation during inflation. (For a discussion of pure Yukawa interaction involving massless fermions in a locally de Sitter geometry see Ref. [10]. For a discussion of one-loop effects in chaotic inflation without the Yukawa interaction see Ref. [11].) For convenience, we will set the renormalization scale $\mu = hm_P$, where $m_P \approx 2.4\times10^{18}$ GeV is the (reduced) Planck scale. (Changing the renormalization scale corresponds to redefining λ, and does not affect the physics.)

The instability for $\phi \gg m_P$ caused by the negative contribution of Eq. (1) will not concern us too much here. Presumably it is taken care of in a more fundamental theory. Our inflationary phase takes place for ϕ values below the local maximum. Although this differs from the original chaotic inflation model, it is still possible to justify the initial conditions. Inflation most naturally starts at an energy density close to the Planck scale. However, the observable part of inflation occurs at a much lower energy density. If, after the initial phase of inflation, there exist regions of space where the field is sufficiently close to the local maximum, eternal inflation takes place. It would then seem that the regions satisfying the condition for eternal inflation would always dominate, since even if they are initially rare, their volume will increase indefinitely. For discussions of this point, see e.g. Refs. [7, 12, 13].

Before we discuss the effect of Eq. (1) on the inflationary parameters, let's recall the basic equations. The slow-roll parameters may be defined as (see Ref. [14] for a review and references):

$$\epsilon = \frac{1}{2}\left(\frac{V'}{V}\right)^2, \quad \eta = \frac{V''}{V}, \quad \xi^2 = \frac{V'V'''}{V^2}\,. \tag{5}$$

Here and below we use units $m_P = 1$, and '$\prime$' denotes derivative with respect to ϕ. The spectral index n_s, the tensor to scalar ratio r and the running of the spectral index $\alpha \equiv {\rm d}n_s/{\rm d}\ln k$ are given by

$$n_s = 1 - 6\epsilon + 2\eta\,, \tag{6}$$
$$r = 16\epsilon\,, \tag{7}$$
$$\alpha = 16\epsilon\eta - 24\epsilon^2 - 2\xi^2\,. \tag{8}$$

The amplitude of the curvature perturbation Δ_R is given by

$$\Delta_R = \frac{1}{2\sqrt{3}\pi}\frac{V^{3/2}}{|V'|}\,. \tag{9}$$

The WMAP best fit value for the comoving wavenumber $k_0 = 0.002$ Mpc^{-1} is $\Delta_R = 4.91\times10^{-5}$ [2].

In the slow-roll approximation, the number of e-folds is given by

$$N_0 = \int_{\phi_e}^{\phi_0}\frac{V{\rm d}\phi}{V'}\,, \tag{10}$$

where the subscript '0' implies that the values correspond to k_0. The subscript 'e' implies the end of inflation, where $\epsilon(\phi_e) \simeq 1$. N_0 corresponding to the same scale is [15]

$$N_0 \approx 65 + \frac{1}{2}\ln[V(\phi_0)] - \frac{1}{3\gamma}\ln[V(\phi_e)] + \left(\frac{1}{3\gamma}-\frac{1}{4}\right)\ln[\rho_{\rm reh}]\,, \tag{11}$$

where $\rho_{\rm reh}$ is the energy density at reheating, and $\gamma - 1$ represents the average equation of state during oscillations of the inflaton. For $V \propto \phi^n$, $\gamma = 2n/(n+2)$ [16]. In particular, for ϕ^2 inflation $\gamma = 1$ and the universe expands as matter dominated during inflaton oscillations, whereas for ϕ^4 inflation $\gamma = 4/3$ and the universe expands as radiation dominated. In the latter case N_0 does not depend on $\rho_{\rm reh}$. Note that with quantum corrections included in the potential, γ will in principle deviate from its tree level value. However this effect is quite negligible since the tree level term dominates at low values of ϕ where inflation has ended.

First, assume that $\lambda \ll m^2/\phi^2$ during inflation, so that inflation is primarily driven by the quadratic ϕ^2 term. For the tree level potential $V = (1/2)m^2\phi^2$, Eq. (10) gives $N_0 \simeq \phi_0^2/4$. Using Eq. (9), $m \simeq 1.6\times10^{13}$ GeV. Using the above definitions we also obtain

$$n_s = 1 - 8/\phi^2 = 1 - 2/N\,, \tag{12}$$
$$r = 32/\phi^2 = 8/N\,, \tag{13}$$
$$\alpha = -32/\phi^4 = -2/N^2\,. \tag{14}$$

The number of e-folds is given by Eq. (11). Assuming $m_N \ll m$, the inflaton decay rate $\Gamma_\phi = h^2m/(8\pi)$ (where $h^2 < m$) and $\rho_{\rm reh} \simeq \kappa m^2 m_P^2$.

We can simplify the discussion of the potential with the loop correction by treating $\ln\phi$ as constant. We then have

$$V = \frac{1}{2}m^2\phi^2 - \kappa\phi^4\ln\phi\,, \tag{15}$$
$$V' \simeq m^2\phi - 4\kappa\phi^3\ln\phi\,, \tag{16}$$
$$\Delta_R \simeq \frac{1}{4\sqrt{3}\pi}\sqrt{\kappa}\phi^3\frac{(u+1)^{3/2}}{u}\,, \tag{17}$$

where in Eq. (17) we have defined

$$u \equiv \frac{m^2}{2\kappa\phi^2\ln\phi} - 2\,. \tag{18}$$

TABLE I: The inflationary parameters for the potential $V = (1/2)m^2\phi^2 - \kappa\phi^4 \ln(\phi/m_P)$ (in units $m_P = 1$)

$\log_{10}(\kappa)$	m (10^{-6})	ϕ_e	ϕ_0	$V(\phi_0)^{1/4}$	N_0	u_0	n_s	r	α (10^{-4})
$V = (1/2)m^2\phi^2$ (assuming $\rho_{\rm reh} = 10^{-16}m^2m_P^2$)									
	6.437	1.457	15.26	0.008334	58.31		0.9657	0.1349	-5.901
ϕ^2 branch									
-16	6.434	1.457	15.25	0.008322	58.31	319.4	0.9657	0.1341	-5.901
-15	6.383	1.457	15.15	0.008204	58.47	30.2	0.9656	0.1267	-5.853
-14.5	6.245	1.457	14.83	0.007891	58.5	8.355	0.9645	0.1085	-5.647
-14.2	5.798	1.457	14.19	0.007212	58.43	3.165	0.9591	0.07567	-4.423
-14.11	4.917	1.456	13.35	0.006241	58.23	2.067	0.9459	0.04239	-1.254
Hilltop branch									
-14.11	4.917	1.456	13.35	0.006241	58.23	2.067	0.9459	0.04239	-1.254
-14.2	3.628	1.456	12.35	0.005019	57.93	0.3324	0.9219	0.01769	3.196
-14.5	2.146	1.455	11.18	0.003603	57.48	0.1447	0.8852	0.004665	6.022
-15	1.032	1.455	10.04	0.002344	56.88	0.0531	0.8424	0.000826	5.236
-16	0.268	1.453	8.617	0.001103	55.86	0.0102	0.7762	0.000039	2.254

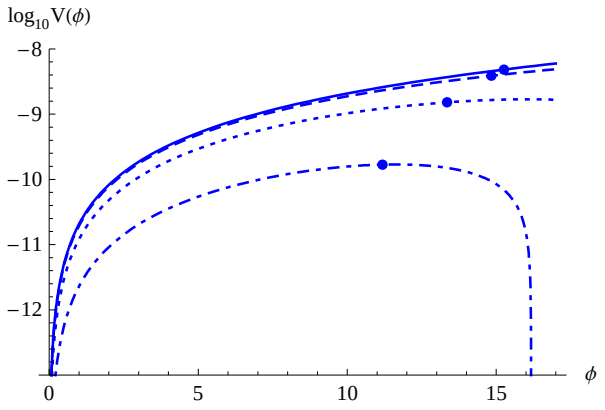

FIG. 1: The tree level potential (solid), the ϕ^2 and hilltop solution potentials for $\log_{10}(\kappa) = -14.5$ (dashed and dot-dashed), and the potential for $\log_{10}(\kappa) = -14.11$ where the two solutions meet (dotted). The points on the curves denote ϕ_0.

The inflationary parameters are given by

$$n_s \simeq 1 - \frac{8}{\phi^2}\left[\frac{u^2+(3/2)u+2}{(u+1)^2}\right], \quad (19)$$

$$r \simeq \frac{32}{\phi^2}\left[\frac{u^2}{(u+1)^2}\right], \quad (20)$$

$$\alpha \simeq -\frac{32}{\phi^4}\left[\frac{u(u^3+3u^2+2u-3)}{(1+u)^4}\right]. \quad (21)$$

The numerical solutions are obtained (without the constant $\ln\phi$ approximation, except for calculating u_0) using Eq. (9), Eq. (10) and Eq. (11). (We also include the next to leading order corrections in the slow roll expansion, see Appendix.) One way to obtain the solutions is to fix κ and scan over m (with ϕ_0 calculated for each m value using Eq. (9)) until N_0 matches Eq. (11). There are two solutions for a given value of κ. From Eq. (17), in the large u_0 limit ($u_0 \gg 1$ or $m^2 \gg 4\kappa\phi_0^2\ln\phi_0$) a solution is obtained with $\kappa \propto 1/u_0$. In the small u_0 limit ($u_0 \ll 1$ or $m^2 \approx 4\kappa\phi_0^2\ln\phi_0$), $\kappa \propto u_0^2$. The two solutions meet at $u_0 \sim 1$, giving a maximum value of $\kappa \sim (\sqrt{6}\pi\Delta_R)^2/\phi_0^6$. For larger values of κ, it is not possible to satisfy the Δ_R and N_0 constraints simultaneously, since the duration of inflation becomes too short for the lower ϕ_0 values required to keep Δ_R fixed.

We call the large u_0 solution the ϕ^2 solution, and the other the hilltop solution [13]. For the ϕ^2 solution, $u_0 \to \infty$ as $\kappa \to 0$. The predictions for $V = (1/2)m^2\phi^2$ are recovered for $u_0 \gg 1$. On the other hand, for the hilltop solution $u_0 \to 0$ as $\kappa \to 0$. With $u_0 \ll 1$, $n_s \approx 1 - 16/\phi_0^2$ and r is suppressed by u^2. For the ϕ^2 solution the local maximum of the potential and ϕ_0 is at higher values, whereas for the hilltop solution inflation occurs closer to the local maximum (see Fig. 1 and Table I). As the value of κ is increased, the two branches of solutions approach each other and they meet at $\kappa \simeq 8\times10^{-15}$ (see Fig. 2).

Note that the one loop contribution to λ is of order $(4!)\kappa$, which is $\sim m^2/\phi^2$ in the parameter range where the κ term has a significant effect on inflationary observables. In this case our assumption $\lambda \ll m^2/\phi^2$ corresponds to the renormalized coupling being small compared to the one loop contribution.

Alternatively, assume that $\lambda \gg m^2/\phi^2$ during inflation, so that inflation is primarily driven by the quartic term. For the tree level potential $V = (1/4!)\lambda\phi^4$, Eq. (10) gives $N_0 \simeq \phi_0^2/8$. Using Eq. (9), $\lambda \simeq 8\times10^{-13}$. We also obtain

$$n_s = 1 - 24/\phi^2 = 1 - 3/N, \quad (22)$$

$$r = 128/\phi^2 = 16/N, \quad (23)$$

$$\alpha = -192/\phi^4 = -3/N^2. \quad (24)$$

TABLE II: The inflationary parameters for the potential $V = (1/4!)\lambda\phi^4 - \kappa\phi^4 \ln(\phi/m_P)$ (in units $m_P = 1$)

$\log_{10}(\kappa)$	$\log_{10}(\lambda)$	ϕ_e	ϕ_0	$V(\phi_0)^{1/4}$	N_0	v_0	n_s	r	α (10^{-4})
				$V = (1/4!)\lambda\phi^4$					
	-12.07	2.53	22.39	0.009737	62.55		0.9517	0.251	-7.637
				ϕ^4 branch					
-15.	-12.03	2.516	22.31	0.00972	62.54	143.1	0.9519	0.2493	-7.606
-14.	-11.78	2.438	21.69	0.009558	62.43	14.08	0.9539	0.2331	-7.372
-13.5	-11.49	2.369	20.49	0.009058	62.2	3.834	0.9575	0.1881	-7.025
-13.3	-11.36	2.338	19.35	0.008344	61.97	1.762	0.9577	0.1355	-6.261
-13.24	-11.33	2.319	18.23	0.007421	61.74	0.9184	0.9512	0.08476	-3.725
				Hilltop branch					
-13.24	-11.33	2.319	18.23	0.007421	61.74	0.9184	0.9512	0.08476	-3.725
-13.3	-11.41	2.305	17.11	0.006329	61.49	0.4937	0.9359	0.04481	0.9321
-13.5	-11.63	2.292	15.85	0.004985	61.14	0.2391	0.9088	0.01718	6.326
-14.	-12.15	2.276	14.15	0.003225	60.57	0.0799	0.8618	0.002978	8.232
-15.	-13.18	2.256	12.15	0.001534	59.69	0.0151	0.7959	0.000149	4.078

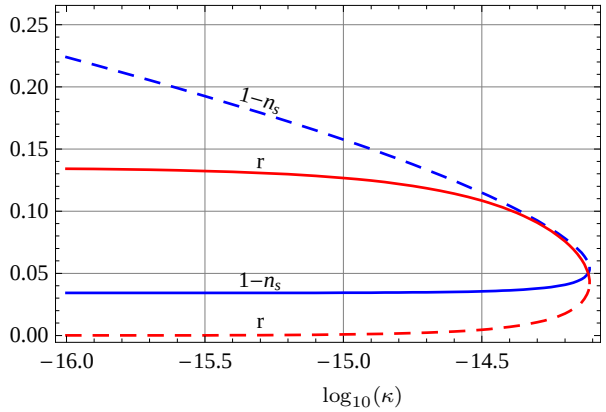

FIG. 2: $1 - n_s$ and r vs. κ for the potential $V = (1/2)m^2\phi^2 - \kappa\phi^4 \ln(\phi/m_P)$. Solid and dashed curves correspond to ϕ^2 and hilltop branches respectively.

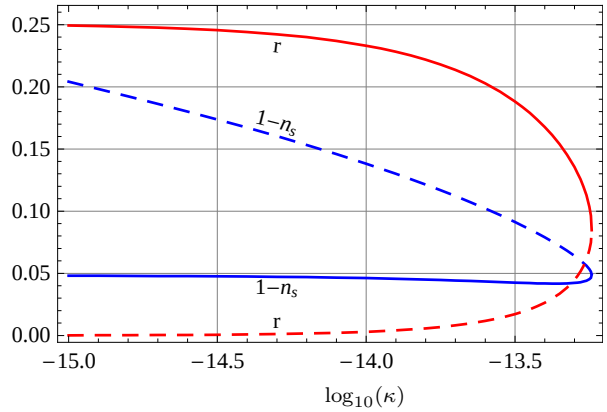

FIG. 3: $1 - n_s$ and r vs. κ for the potential $V = (1/4!)\lambda\phi^4 - \kappa\phi^4 \ln(\phi/m_P)$. Solid and dashed curves correspond to ϕ^4 and hilltop branches respectively.

Including the loop correction we have

$$V = \frac{\phi^4}{24}(\lambda - 24\kappa \ln\phi)\,, \tag{25}$$

$$V' = \frac{\phi^3}{6}(\lambda - 6\kappa - 24\kappa \ln\phi)\,, \tag{26}$$

$$\Delta_R \simeq \frac{\sqrt{3}}{48\pi}\sqrt{\kappa}\phi^3\frac{(v+1)^{3/2}}{v}\,, \tag{27}$$

where in Eq. (27) we have defined

$$v \equiv \frac{1}{6\kappa}(\lambda - 6\kappa - 24\kappa \ln\phi)\,. \tag{28}$$

The inflationary parameters are given by

$$n_s = 1 - \frac{24}{\phi^2}\left[\frac{v^2 + v/3 + 4/3}{(v+1)^2}\right]\,, \tag{29}$$

$$r = \frac{128}{\phi^2}\left[\frac{v^2}{(v+1)^2}\right]\,, \tag{30}$$

$$\alpha = -\frac{192}{\phi^4}\left[\frac{v(v^3 + (4/3)v^2 + 5v - 10/3)}{(1+v)^4}\right]\,. \tag{31}$$

The numerical results are displayed in Fig. 3 and Table II. As before, there are two solutions for a given value of κ. We call the large v_0 solution the ϕ^4 solution, and the other the hilltop solution. The predictions for $V = (1/4!)\lambda\phi^4$ are recovered for $v_0 \gg 1$, or $\lambda \gg 24\kappa \ln\phi_0$. Since $\phi_0^2 = 8N_0$ for ϕ^4 potential, this corresponds to $\lambda \gg 75\kappa$. As the value of κ is increased, the two branches of solutions approach each other and they meet at $\kappa \simeq (4\sqrt{6}\pi\Delta_R)^2/\phi_0^6 \simeq 6 \times 10^{-14}$.

To summarize, in this paper we have considered the impact radiative corrections can have on chaotic inflation predictions with ϕ^2 and ϕ^4 potentials. A Yukawa coupling of ϕ, in particular, induces corrections to the in-

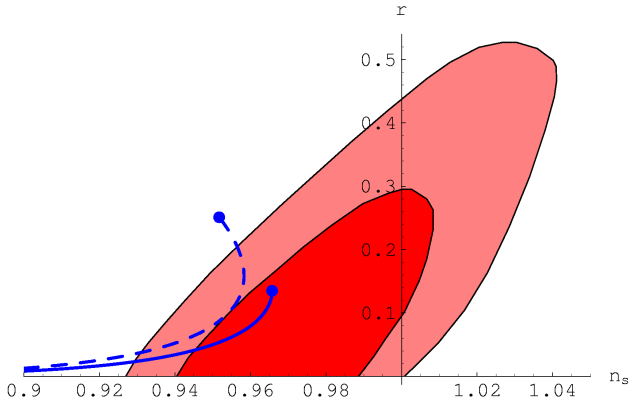

FIG. 4: Tensor to scalar ratio r vs. the spectral index n_s for the potential $V = (1/2)m^2\phi^2 - \kappa\phi^4 \ln(\phi/m_P)$ (solid curve) and for the potential $V = (1/4!)\lambda\phi^4 - \kappa\phi^4 \ln(\phi/m_P)$ (dashed curve). The WMAP contours (68% and 95% CL) are taken from Ref. [2]. The points on the curves correspond to the tree level predictions for ϕ^2 and ϕ^4 potentials.

flationary potential with a negative sign, which can lower r. We display the possible range of values for the inflationary parameters including such corrections. As shown in Fig. 4, although ϕ^4 inflation seems excluded at tree level, it can become compatible with WMAP when this correction is included. The current WMAP limits imply $r \gtrsim 0.02$ ($r \gtrsim 0.04$) for the ϕ^2 (ϕ^4) model, which therefore suggests that signatures of primordial gravitational waves should be observed in the near future.

Finally we note that radiative corrections can also significantly alter the inflationary predictions of other models. For instance, the Yukawa coupling induced correction considered here can lead to a red-tilted spectrum (including $n_s \approx 0.96$ as favored by WMAP) in the non-supersymmetric hybrid inflation model [17], which otherwise predicts a blue spectrum.

Acknowledgments

This work is partially supported by the US DOE under contract number DE-FG02-91ER40626 (Q.S.).

Appendix

We provide here the next to leading order formulae for calculating n_s and r that we have used [18]:

$$\Delta_R = \frac{1}{2\sqrt{3}\pi}\frac{V^{3/2}}{|V'|}\left[1 - \left(3C + \frac{1}{6}\right)\epsilon + \left(C - \frac{1}{3}\right)\eta\right], \tag{32}$$

$$n_s = 1 + 2\left[-3\epsilon + \eta - \left(\frac{5}{3} + 12C\right)\epsilon^2 + (8C-1)\,\epsilon\eta + \frac{1}{3}\eta^2 - \left(C - \frac{1}{3}\right)\xi^2\right], \tag{33}$$

$$r = 16\epsilon\left[1 + \frac{2}{3}(3C-1)(2\epsilon - \eta)\right], \tag{34}$$

where $C = \ln 2 + \gamma_E - 2 \approx -0.7296$. Inflation ends at $\epsilon_H = 1$ and

$$N_0 = \int_{\phi_e}^{\phi_0} \frac{\mathrm{d}\phi}{\sqrt{2\epsilon_H}}, \tag{35}$$

$$\epsilon_H = 2\left(\frac{H'(\phi)}{H(\phi)}\right)^2 = \epsilon\left(1 - \frac{4}{3}\epsilon + \frac{2}{3}\eta + \frac{32}{9}\epsilon^2 + \frac{5}{9}\eta^2 - \frac{10}{3}\epsilon\eta + \frac{2}{9}\xi^2 + \ldots\right). \tag{36}$$

[1] A. D. Linde, Phys. Lett. **B129**, 177 (1983).
[2] J. Dunkley et al. (WMAP), arXiv:0803.0586.
[3] E. Komatsu et al. (WMAP), arXiv:0803.0547.
[4] S. R. Coleman and E. Weinberg, Phys. Rev. **D7**, 1888 (1973).
[5] Q. Shafi and V. N. Şenoğuz, Phys. Rev. **D73**, 127301 (2006) [arXiv:astro-ph/0603830].
[6] M. Kawasaki, M. Yamaguchi and T. Yanagida, Phys. Rev. Lett. **85**, 3572 (2000) [arXiv:hep-ph/0004243].
[7] A. D. Linde, *Particle Physics and Inflationary Cosmology* (Chur, Switzerland: Harwood, 1990) [arXiv:hep-th/0503203].
[8] A. D. Linde, Lect. Notes Phys. **738**, 1 (2008) [arXiv:0705.0164].
[9] D. Cirigliano, H. J. de Vega and N. G. Sanchez, Phys. Rev. **D71**, 103518 (2005) [arXiv:astro-ph/0412634]. Also see R. Kallosh and A. Linde, JCAP **0704**, 017 (2007) [arXiv:0704.0647] and references therein.
[10] S.-P. Miao and R. P. Woodard, Phys. Rev. **D74**, 044019 (2006) [arXiv:gr-qc/0602110].
[11] M. S. Sloth, Nucl. Phys. **B748**, 149 (2006) [arXiv:astro-ph/0604488]; Nucl. Phys. **B775**, 78 (2007) [arXiv:hep-th/0612138].
[12] A. Vilenkin, Phys. Rev. **D27**, 2848 (1983).
[13] L. Boubekeur and D. H. Lyth, JCAP **0507**, 010 (2005) [arXiv:hep-ph/0502047].
[14] A. R. Liddle and D. H. Lyth, *Cosmological inflation and large-scale structure* (Cambridge, UK: Univ. Pr., 2000).
[15] E. W. Kolb and M. S. Turner, *The Early universe* (Addison-Wesley, 1990); A. R. Liddle and S. M. Leach, Phys. Rev. **D68**, 103503 (2003) [arXiv:astro-ph/0305263].
[16] M. S. Turner, Phys. Rev. **D28**, 1243 (1983).
[17] A. D. Linde, Phys. Rev. **D49**, 748 (1994) [arXiv:astro-ph/9307002].
[18] E. D. Stewart and D. H. Lyth, Phys. Lett. **B302**, 171 (1993) [arXiv:gr-qc/9302019]; E. W. Kolb and S. L. Vadas, Phys. Rev. **D50**, 2479 (1994) [arXiv:astro-ph/9403001]; A. R. Liddle, P. Parsons, and J. D. Barrow, Phys. Rev. **D50**, 7222 (1994) [arXiv:astro-ph/9408015].